Low Complexity Methods for Joint Detection and Synchronization of TDMA Bursts

Haotian Zhai and Bernd-Peter Paris
Department of Electrical and Computer Engineering
George Mason University
Fairfax, VA 22030
{hzhai,pparis}@gmu.edu

***Abstract*—This paper proposes a data-aided joint detection and carrier synchronization algorithm for TDMA bursts. A sequential detection algorithm based on the generalized likelihood ratio test (GLRT) is used to detect the embedded preamble signal in received data stream. Carrier synchronzation happens during sequential detection to provide carrier estimates for GLRT and after detection to compute accurate estimates for coherent demodulation. Thus, we propose a family of estimators with low-complexity and high-accuracy to accommodate for the two cases. At the end, the complete joint detection and estimation algorithm is validated through simulation and SDR at a very high sample rate.**

I. Introduction

In digital communication systems, information is commonly transmitted in time-multiplexed bursts. Examples include time-slotted random access systems. Each active user transmits information to the receiver in the same frequency band and in non-overlapping time intervals [1]. A fundamental prerequisite for successful coherent demodulation is that the receiver can detect the beginning of the data stream and estimate accurately the phase and frequency offset of the carrier. It is worth emphasizing that time and carrier synchronization are coupled problems, especially at low SNRs: coherent methods for detecting the signal require accurate frequency and phase estimates while data-aided frequency and phase estimation requires that the location of the training sequence is available. Thus, joint signal detection and carrier synchronization algorithms play a vital role in any communication system.

Clearly, the signal acquisition problem has been considered widely. In the late 90's, Morelli and Mengali [2] presented a tutorial review of the carrier synchronization field comparing such characteristics as estimation accuracy, range, and computational complexity of available techniques. The work by [3]–[5] is most related to results in this paper. For signal detection, particularly, sequential detection process, most of the sequential detector is built based on hypothesis testing [6]–[8]. Moreover, the lack of information happens commonly when build likelihood ratio test (LRT). For example, the LRT in [7] is built based on the distribution of data stream, which is unknown. The LRT is then replaced by generalized likelihood ratio test.

In this paper, we propose a joint detection and estimation algorithm for the signal acquisition process and implement it on software-defined radio (SDR). In particular, the detection algorithm operates sequentially for every incoming sample and is built based on the estimates from the carrier synchronization.

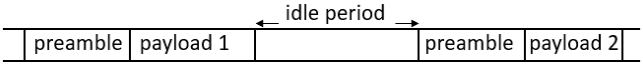

Fig. 1. Structure of signal stream at the receiver

Thus, a family of low-complexity and high-accuracy estimators is proposed for implementing in sequential detection and coherent demodulation on SDR at very high sample rate.

II. Signal Model

In an uplink multiuser system, the transmitted signal frame from each user is seperated by an unkown length of idle period and assumed to include a reference signal that is known to the receiver. Often such a reference sequence is prepended to the payload and is referred to as a preamble. The structure of signal stream at the receiver is shown in Figure 1. The problem addressed in this paper is to accurately estimate the start time of the preamble and to estimate carrier phase and frequency offset from the preamble. Hence, the payload portion of the frame is not further considered.

We now give the signal model for this paper. The received RF signal is first modulated by base band; In [2], [6], the authors then got a simplifed signal model from the matched filter by assuming the symbol time is perfectly known. However, in practice, this is unreliable at low SNR. To accommodate this issue, we analyze the discrete signal model directly after modulation and sampler, which is given by

$$r_n = s_{n-p} A e^{j\phi} e^{j2\pi\delta n} + w_n, \tag{1}$$

where s_n denotes the sampled received reference sequence (the preamble), which has the form

$$s_n = \sum_{i=0}^{L_0-1} c_i g(nT_s - iT) \quad \text{for } n = 0, \ldots, N-1, \tag{2}$$

In (1), p denotes the start position of the received preamble. Note, because of the uncertainty of sampling, often the sampler may not sample exactly at the start time of the preamble, which causes the integer delay p with a fractional delay in the range of $[-\frac{T_s}{2}, \frac{T_s}{2})$, where T_s is the sample period as in (2). However, since we are considering the signal transmission in burst mode, i.e., the data rate is very high, the effect of the fractional delay

can be ignored for this paper. A, ϕ, δ are the amplitude, carrier phase and normalized frequency offset with respect to sample period T_s that we want to estimate. w_n is the complex AWGN of variance N_0/E_s. Thus, E_s/N_0 denotes the ratio of signal energy to noise power spectral density (SNR).

In (2), T denotes the symbol period and $g(t)$ provides pulse shaping. $\{c_i\}_{i=0}^{L_0-1}$ is the known symbol sequence at transmitter and receiver, where L_0 denotes the number of symbols. We further define M to be the rate of oversampling in each symbol, thus $M = \frac{T}{T_s}$, and $N = ML_0$ is the number of samples in the preamble. Note, compared with the signal model in [2], [6], [9], by using the extra oversampled samples per symbol, our signal model is not limited to small frequency offsets.

III. Detection and Time Synchronization

We start by looking at the two hypotheses for the sequential detection task: Let H_0 be the null hypothesis that the received signal is the channel noise or only contains a portion of the preamble against the alternative H_1 that it contains the entire preamble. Define Δ to be the distance between the current start position of the observation of N received samples and the start position of the preamble (p). Thus, for $n = 0, 1, \ldots, N-1$, the two hypotheses are given by

$$\begin{aligned} H_0 :\ r_n &= \begin{cases} s_{n-\Delta} A e^{j\phi} e^{j2\pi\delta(n-\Delta)} + w_n & \text{for } \Delta \in (0, N-1], \\ w_n & \text{otherwise,} \end{cases} \\ H_1 :\ r_n &= s_n A e^{j\phi} e^{j2\pi\delta n} + w_n. \end{aligned} \tag{3}$$

Note, in [6]–[8], the authors define hypothesis H_0 only when no preamble is observed. Although, in [7], the author points out the effect of partial preamble can be kindly avoided by using the preamble symbol sequence with a good autocorrelation property. In this paper, we still focus on discussing when partial preamble is observed because it is the worst case of H_0 and it affects the result of hypothesis testing.

Based on the above discussion, we now build the conditional likelihood ratio test (CLRT) between H_0 under $\Delta \in (0, N-1]$ and H_1 by giving the distance Δ, the phasor $\xi = Ae^{j\phi}$ and the frequency offset δ at the position of the preamble (we omit discussing CLRT for $H_0 : r_n = w_n$, since it is a traditional and well-known hypothesis testing problem). The hypothesis testing is given by

$$\begin{aligned} \Lambda(R|\Delta,\xi,\delta) &= \frac{f_{R|H_1,\xi,\delta}(r|H_1,\xi,\delta)}{f_{R|H_0,\Delta,\xi,\delta}(r|H_1,\Delta,\xi,\delta)} \\ &= \frac{\prod_{n=0}^{N-1} \frac{1}{\sqrt{\pi N_0}} e^{-\frac{|r_n - s_n \xi e^{j2\pi\delta n}|^2}{N_0}}}{\frac{1}{(\pi N_0)^{N/2}} \prod_{n=\Delta}^{N-1} e^{-\frac{|r_n - s_{n-\Delta}\xi e^{j2\pi\delta(n-\Delta)}|^2}{N_0}} \prod_{n=0}^{\Delta-1} e^{-\frac{|r_n|^2}{N_0}}} \\ &\underset{H_0}{\overset{H_1}{\gtrless}} \eta. \end{aligned} \tag{4}$$

Cancelling the common parts and taking the logarithm, (4) is reduced to

$$\Re\left\{ \sum_{n=0}^{N-1} r_n s_n^* \xi^* e^{-j2\pi\delta n} - \sum_{n=\Delta}^{N-1} r_n s_{n-\Delta}^* \xi^* e^{-j2\pi\delta(n-\Delta)} \right\} \underset{H_0}{\overset{H_1}{\gtrless}} \frac{N_0}{2} \ln\eta + \frac{A^2}{2} \sum_{n=N-\Delta}^{N-1} |s_n|^2. \tag{5}$$

Note, on the left hand side, the two summations perform like the matched filter for hypothesis H_1 and H_0, respectively. To explain this, we plug $r_n = s_n \xi e^{j2\pi\delta n} + w_n$ under hypothesis H_1 into the left hand side of (5). In the real operator, it yields

$$A^2 \sum_{n=0}^{N-1} |s_n|^2 - A^2 e^{j2\pi\delta\Delta} \sum_{n=\Delta}^{N-1} s_n s_{n-\Delta}^* + \text{zero-mean noise}, \tag{6}$$

where $A^2 \sum_{n=0}^{N-1} |s_n|^2$ denotes the energy of the preamble and $\sum_{n=\Delta}^{N-1} s_n s_{n-\Delta}^*$ is the "partial" autocorrelation function (ACF) of the preamble at lag Δ. Similarly, it can be derived the left hand side of (5) under hypothesis H_0 in the real operator is

$$-A^2 \sum_{n=\Delta}^{N-1} |s_{n-\Delta}|^2 + A^2 e^{-j2\pi\delta\Delta} \sum_{n=\Delta}^{N-1} s_{n-\Delta} s_n^* + \text{zero-mean noise}. \tag{7}$$

Thus, based on (6) and (7), we can conclude that the principle value of the log-CLRT reduces to the difference between the energy of the (partial) preamble and the ACF of the preamble sequence at lag Δ. By using the symbol sequence $\{c_i\}$ of s_n with a good autocorrelation property, e.g., Gold sequence, the effect of the ACF can be kindly mitigated; However, because of pulse shaping, the autocorrelation property of the preamble is decreased so that the effect of the ACF cannot be ignored.

In practice, the distance Δ is an unknown information to the receiver, which means the second summation of (5) is not computable. However, the first summation is computable and it reflects the energy of the preamble under H_1 and the "partial" ACF under H_0. Thus, a practical sequential detector is built just based on the classical cross-correlation between the received signal and the preamble corrected by the frequency and phasor estimates with some proper scaling. Specifically,

$$\rho(\tilde{p}) = \frac{\Re\{\langle \boldsymbol{r}_{\tilde{p}}, \hat{\boldsymbol{s}}_{\tilde{p}} \rangle\}}{||\boldsymbol{r}_{\tilde{p}}|| \cdot ||\hat{\boldsymbol{s}}_{\tilde{p}}||} \underset{H_0}{\overset{H_1}{\gtrless}} \gamma \tag{8}$$

where $\tilde{p}$=p+Δ denotes the general start position of received signal. $\boldsymbol{r}_{\tilde{p}}$=$[r_{\tilde{p}}, r_{\tilde{p}+1}, \ldots, r_{\tilde{p}+N-1}]$ represents the received signal sequence at the position $\tilde{p}$, and $\hat{\boldsymbol{s}}_{\tilde{p}}$ represents the carrier-estimates corrected preamble sequence, where each element is $\hat{s}_n = s_n \hat{\xi}_{\tilde{p}} e^{j2\pi\hat{\delta}_{\tilde{p}} n}$ for $n = 0, 1, \ldots, N-1$, and $\hat{\xi}_{\tilde{p}}$, $\hat{\delta}_{\tilde{p}}$ are the phasor and frequency estimates at position $\tilde{p}$. Moreover, $||\cdot||$ is the Euclidean norm of the signal sequence, and γ is the normalized detection threshold which lies on the range of $[0, 1]$. From (8), it is obvious that to implement the sequential detector, we need the information of the frequency and

phasor estimates at that position. Thus, a realistic generalized likelihood ratio test (GLRT) replaces the CLRT of (4) by first doing carrier synchronization at each position of detection then plugging the estimates into the LRT. Furthermore, it should be emphasized that our sequential detector requires to work at high sample rate; Although (8) is already the simpliest form, the complexity of the two estimates $\hat{\xi}$,$\hat{\delta}$ is also crucial. A pair of low-complexity frequency and phasor estimates will be given in the next section.

IV. Frequency and Phase Estimation

In this section, we discuss the carrier synchronization problem by assuming the known start time of the preamble in the received sequence. For estimating the frequency offset δ and phasor $\xi = Ae^{j\phi}$, the maximum likelihood estimation (MLE) of the parameters in (1) is given by

$$\hat{\delta}, \hat{\xi} = \min_{\delta, \xi = Ae^{j\phi}} \sum_{n=0}^{N-1} |r_n - s_n \xi e^{j2\pi\delta n}|^2. \tag{9}$$

A closed form for $\hat{\xi}$ is readily derived by taking the Wirtinger derivative with ξ and setting it equal to zero,

$$\hat{\xi} = \frac{\sum_{n=0}^{N-1} r_n s_n^* e^{-j2\pi\hat{\delta}n}}{\sum_{n=0}^{N-1} |s_n|^2}, \tag{10}$$

so that $\hat{\xi}$ relies on the frequency estimate $\hat{\delta}$, and $\hat{\phi} = \arg\{\hat{\xi}\}$.

A necessary condition for the frequency offset estimate $\hat{\delta}$, denoted as $J(\hat{\delta})$, is obtained similarly by taking the derivative of (9) with respect to δ and setting it equal to zero. Skipping all intermediate derivation steps for brevity's sake, it yields

$$J(\hat{\delta}) = \Im\left\{ \sum_{k=1}^{N-1} \sum_{m=k}^{N-1} k r_{m-k} r_m^* s_{m-k}^* s_m e^{j2\pi\hat{\delta}k} \right\} = 0. \tag{11}$$

Note, there are a number of local minima of (9) also satisfying the necessary condition for $\hat{\delta}$ of (11) in addition to the absolute minimum (the exact solution of MLE). In [5] and [4], the "false minima" are avoided by appropriately restricting the operating range of the estimator. Specifically, instead of calculating the sample autocorrelation functions for entire lag $k \in [1, N-1]$, they truncate (11) by only considering the lag autocorrelation functions for $k \in [1, J]$, where $J \ll N-1$. This is due to when k is large, the number of autocorrelation functions is small for averaging, so that (11) produces a poor estimate for $\hat{\delta}$.

Moreover, note that the estimator $\hat{\delta}$ in (11) has no closed-form solution. In [5], the necessary condition is approximated by replacing the exponential with its Taylor series expansion. In [4], an approximate solution is obtained via Euler's identity for large N. Both L&R [5] and Fitz [4] estimators have computational complexity $O(N^2)$ reflecting the double summation. In [3], the Kay estimator reduces the complexity from $O(N^2)$ to $O(N)$ by only computing (11) at lag $k = 1$. However, it suffers a bad accuracy at low SNRs.

In this paper, we propose a family of alternative solutions to (11). A coarse solution with $O(N)$ complexity is used for operating at high sample rate during the sequential detection; It prioritizes low complexity at the expense of some loss of accuracy. A second fine solution is used to improve the estimation accuracy at moderate complexity for coherent demodulation once the preamble has been detected.

A. Coarse Solution: Single-Lag Estimator with Length-v Partial Correlating

The first estimator is rooted in the insight that at high SNR, every lag k in (11) can be used to approximate the frequency estimate δ. By plugging $r_m \approx s_m \xi e^{j2\pi\delta m}$, (11) is expanded to

$$\Im\left\{ A^2 \sum_{k=1}^{N-1} \sum_{m=k}^{N-1} k |s_{m-k}|^2 |s_m|^2 e^{j2\pi(\hat{\delta}-\delta)k} \right\} = 0. \tag{12}$$

Note, the inner summation in (12) is purely real for every lag k if $\hat{\delta} = \delta$. This suggests that an unbiased estimate of $\hat{\delta}$ can be obtained by using only a single lag k. The approach yields a closed-form solution for $\hat{\delta}$. Next, we will show that by using a so-called length-v coherent integrator, the single-lag estimator also gains a good accuracy at low SNRs.

1) Closed-form expression: The single-lag (SL) estimator with length-v partial correlating is given by

$$\hat{\delta}_{SL}^{(v)}(k_v) = -\frac{\arg\left\{ \sum_{l=k_v}^{N/v-1} F_l^* F_{l-k_v} \right\}}{2\pi k_v v}, \tag{13}$$

where F denotes the coherent integrator, and

$$F_l = \sum_{n=lv}^{(l+1)v-1} r_n s_n^*, \quad \text{for } l = 0, 1, \ldots, N/v-1. \tag{14}$$

In (14), v is the number of coherent correlations for averaging in each coherent integrator. Normally, v is set to be a factor of N to include all the sample instants. In (13), k_v denotes the distance between two coherent integrators for calculating the frequency estimate from non-coherent sample instants; $k_v = \lfloor k/v \rfloor$, where $\lfloor \cdot \rfloor$ is the floor operation. Particularly, when v=1, meaning no partial correlating is used, (13) reduces to

$$\hat{\delta}_{SL}^{(1)}(k) = -\frac{\arg\left\{ \sum_{m=k}^{N-1} r_{m-k} r_m^* s_{m-k}^* s_m \right\}}{2\pi k}, \tag{15}$$

which is exactly the closed-form solution for $\hat{\delta}$ to (12) with single lag k.

2) Performance of single-lag estimator: For evaluating the performance of the SL estimator, we first look at the probability density function (PDF) for the two coherent integrators in (13). By plugging $r_n = s_n \xi e^{j2\pi\delta n} + w_n$ into (14), each of the two coherent integrators in (13) yields a complex Gaussian random variable (r.v.) with PDF

$$\begin{aligned} F_l^* &\sim \mathcal{CN}\left(\frac{E_s \xi^*}{MA^2} \sum_{n=lv}^{(l+1)v-1} e^{-j2\pi\delta n}, v\frac{N_0 E_s}{2MA^2} \right), \\ F_{l-k_v} &\sim \mathcal{CN}\left(\frac{E_s \xi}{MA^2} \sum_{n=(l-k_v)v}^{(l-k_v+1)v-1} e^{j2\pi\delta n}, v\frac{N_0 E_s}{2MA^2} \right). \end{aligned} \tag{16}$$

where $A^2|s_n|^2 \approx E_s/M$ denotes the average energy per sample. Note, F_l^* and F_{l-k_v} are uncorrelated. Based on (16), it is easy to get the product $C_{F_l} = F_l^* F_{l-k_v}$ has a mixed distribution with complex Gaussian and a second kind Bessel function, where the mean $\mu_{C_{F_l}}$ and variance $\sigma^2_{C_{F_l}}$ are given by, respectively

$$\begin{aligned}\mu_{C_{F_l}} &= \frac{E_s^2}{M^2A^2}\sum_{n=lv}^{(l+1)v-1} e^{-j2\pi\delta n}\left(\sum_{m=(l-k_v)v}^{(l-k_v+1)v-1} e^{j2\pi\delta m}\right)\\ &= \frac{E_s^2}{M^2A^2}e^{-j2\pi\delta k_v v}\left(\frac{\sin(\pi\delta v)}{\sin(\pi\delta)}\right)^2, \qquad (17)\\ \sigma^2_{C_{F_l}} &= \underbrace{v^2\frac{N_0^2E_s^2}{4M^2A^4}}_{\text{from Bessel}} + \underbrace{2v\frac{N_0E_s^3}{2M^3A^4}\left(\frac{\sin(\pi\delta v)}{\sin(\pi\delta)}\right)^2}_{\text{from Complex Gaussian}},\end{aligned}$$

where $\frac{\sin(\pi\delta v)}{\sin(\pi\delta)}$ is one of Dirichlet function of δ, which approaches maximum value v at δ=0 and first two zeros at $\delta=\pm 1/v$. Note, both $\mu_{C_{F_l}}$, $\sigma^2_{C_{F_l}}$ are independent of l. Thus, $\sum C_{F_l}$ in the argument operator of (13) also has the mixed distribution with complex Gaussian and a second kind Bessel function.

Recall from (13), the distribution of SL estimator depends on $\arg\{\cdot\}$. It is derived that the full pdf of $\arg\{\zeta\}$, where ζ is complex Gaussian distributed, has a good approximation, valid for moderate SNR, as Gaussian. Specifically,

$$\arg\{\zeta\} \sim \mathcal{N}\big(\angle\mu_\zeta, \sigma_\zeta^2/|\mu_\zeta|^2\big). \qquad (18)$$

The derivation of (18) is omitted due to space constraint. Now we can try to evaluate the performance of SL estimator based on the result of (18). By central limit theorem and assuming a large N, the r.v. followed a distribution of second kind Bessel function is assumed to be complex Gaussian. Thus, an alternative performance evaluation based on the ratio of (absolute) square of mean to variance of $\sum C_{F_l}$ is given by

$$\mathrm{SNR}_{\sum C_{F_l}} = \frac{|\mu_{\sum C_{F_l}}|^2}{\sigma^2_{\sum C_{F_l}}} = \frac{(N/v-k_v)\left(\frac{\sin(\pi\delta v)}{\sin(\pi\delta)}\right)^4}{\frac{v^2}{\mathrm{SNR}_{in}^2}+\frac{2v}{\mathrm{SNR}_{in}}\left(\frac{\sin(\pi\delta v)}{\sin(\pi\delta)}\right)^2}. \qquad (19)$$

where $\mathrm{SNR}_{in} = \frac{2E_s}{MN_0}$. From (19), we first see at low SNRs, the variance of the second Bessel r.v. kills the $\mathrm{SNR}_{\sum C_{F_l}}$. Moreover, compared with no correlating, the length-v partial correlating provides an extra processing gain equaling to $\frac{v+2v\mathrm{SNR}_{in}}{1+2v\mathrm{SNR}_{in}}$ to improve the performance of the SL estimator; Although, the above processing gain obtained directly from (19) is very rough, it basically says the processing gain is affected by the input SNR and increased by v. While at high SNRs, both estimators with or without correlating have the same processing gain from the number of correlations in (13), i.e., $N-k$, when $|\delta|v \ll 1$. When $|\delta|v$ is large, the SL estimator with partial correlating will have a visible degradation of accuracy. Thus, the selection of v trades off the processing gain at low SNRs and the incurred large frequency offset.

Furthermore, based on (15), (17) and (18), the distribution of $\hat{\delta}^{(v)}_{SL}(k_v)$ at moderate SNRs is finally given by

TABLE I
COMPLEXITY OF SINGLE-LAG ESTIMATORS WITH AND WITHOUT PARTIAL CORRELATING (COMPLEX PRODUCTS | ADDITIONS)

	Single Detection	Sequential Detection
$\hat{\delta}^{(1)}_{SL}(k)$	2(N-k) | N-k	N-k+1 | N-k
$\hat{\delta}^{(v)}_{SL}(k_v)$	$(2+\frac{1}{v})$(N-k) | $(2-\frac{1}{v})$(N-k)-1	$(2+\frac{1}{v})$(N-k) | $(2-\frac{1}{v})$(N-k)-1

$$\hat{\delta}^{(v)}_{SL}(k_v) \sim \mathcal{N}\left(\delta, \frac{Mv}{4\pi^2k^2(N/v-k_v)E_s/N_0\left(\frac{\sin(\pi\delta v)}{\sin(\pi\delta)}\right)^2}\right). \qquad (20)$$

Thus, $\hat{\delta}^{(v)}_{SL}(k_v)$ is unbiased. A lower bound for the variance of single-lag estimator at high SNRs is obtained as the variance of (20) when $v = 1$. Moreover, we can see the variance of (20) depends on the value of k_v. The best choice for k_v is to choose $k_v = \lfloor\frac{2N}{3v}\rfloor$ to minimize the variance.

3) Estimation range: The SL estimator may suffer the effect of "aliasing" if $2\pi|\delta|k_v v>\pi$. Thus, a safe estimation range for the estimator with optimal $k_v = \lfloor\frac{2N}{3v}\rfloor$ to avoid the modulo-2π operation is δ within $\pm 3/(4MN)$. Compared with the same autocorrelation-based estimator, e.g., the L&R [5] and Fitz [4], single-lag estimator has 3/8 estimation range of L&R and 3/4 estimation range of Fitz.

4) Computational complexity: We have discussed the accuracy of single-lag estimator. It is also necessary to compare with the complexity since single-lag estimator is used in high sample-rate case. The computational complexity of single-lag estimator can be readily assessed from (13), (14) and (15).

Specifically, we compare with the complexity of SL estimators in single and sequential detection with and without partial correlating. Note, with partial correlating, the SL estimator has same complexity in single and sequential detection since the coherent integrator requires the product of the received samples and the preamble at the same sample instants. However, with no partial correlating, from (15), we see $s^*_{m-k}s_m$ can be precomputed and stored like "filter coefficients"; Moreover, due to the characteristic of the sequential detection process, the products of received samples, $r_{m-k}r^*_m$, can be stored in a shift register so that only one new product needs to be computed per sample period.

The exact computational complexity of two single-lag estimators are given in Table I. We see $\hat{\delta}^{(1)}_{SL}(k)$ has 2 times lower complex products and additions compared with $\hat{\delta}^{(v>1)}_{SL}(k_v)$ in sequential detection. Furthermore, note the complexity of Kay estimator in [2] is given approximately $\frac{3N}{4}$ complex products and additions. By plugging the optimal $k = \frac{2N}{3}$, $\hat{\delta}^{(1)}_{SL}(k)$ finally has a lower complexity than Kay estimator with $\frac{2N}{3}$ complex products and additions.

B. Fine Solution: Newton-Method based Estimator

The principle of Newton-Method based estimator is to use the single-lag estimator as the starting point for a Newton-type iteration aimed at finding a better solution to the necessary

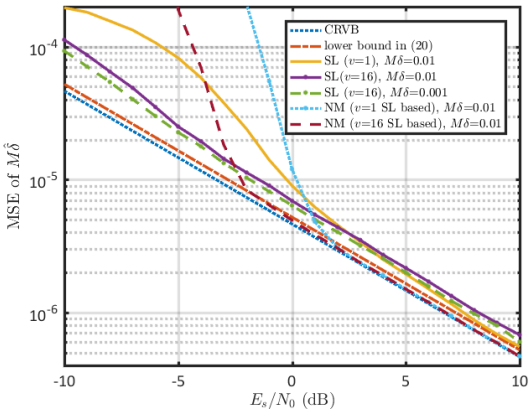

Fig. 2. Accuracy of the NM estimator and single-lag estimator ($L_0 = 32$)

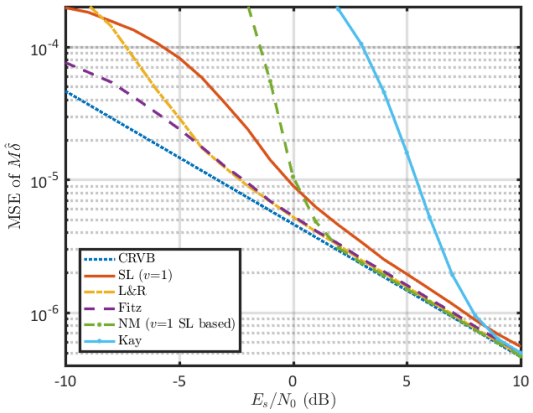

Fig. 3. Accuracy of SL, NM and traditional estimators ($L_0 = 32$, $M\,\delta = 0.01$)

condition (11). In principle, multiple iterations are possible to produce successively better approximations to the root of $J'(\cdot)$ in (11). Specifically, the iterations are given by

$$\hat{\delta}_{NM}^{(i+1)} = \hat{\delta}_{NM}^{(i)} - \frac{J(\hat{\delta}_{NM}^{(i)})}{J'(\hat{\delta}_{NM}^{(i)})} \tag{21}$$

where $\hat{\delta}_{NM}^{(0)} = \hat{\delta}_{SL}^{(v)}(k_v)$ is the starting point of iteration and $J'(\cdot)$ denotes the derivative of J with respect to $\hat{\delta}$. Our simulations indicate that only a single iteration is usually sufficient to achieve very good accuracy.

From (21) and the previous discussion, we can conclude the importance of accuracy of single-lag estimator at low SNRs: with a merely sufficient good accuracy, the single-lag estimator not only increases the probability of detection by better fitting the preamble and received signal as in sequential detector (8), but it provides a reasonable starting point for getting the more accurate NM estimator. In simluations, we will also show the case when the NM estimator has a worse accuracy than single-lag estimator if the latter does not provide enough accuracy.

V. Simulation Results

In simulation section, we reverse the order by first showing the accuracy of estimators in carrier synchronization and then showing some results of sequential detection since the GLRT sequential detector in (8) relies on the accuracy of the single-lag estimator. The symbol sequence of the preamble is chosen as the Gold sequence and modulated by a QPSK alphabet with good autocorrelation properties. The pulse is chosen by 50% rolloff Square-Root Raised Cosine (SRRC) pulse to satisfy the (squared root of) nyquist property. The normalized frequency offset δ is intentionally set to be in the safe estimation range for all estimators for simulation purpose.

A. Simulation Results for Estimation

Figure 2 illustrates the accuracy of single-lag (SL) and the NM estimator. Compared with the two curves of SLs with v=1 and v=16, we see the length-v partial correlating improves the accuracy of SL by providing an approximate 2.5 dB processing gain at negative SNRs. Moreover, the SL with v=1 approaches the lower bound (20) at high SNRs rather than SL with v=16. The gap is due to the Dirichlet function in (20) with respect to v and δ increases the variance. For the same reason, the accuracy of SL with v=16 at small normalized frequency offset has a better accuracy at all SNRs.

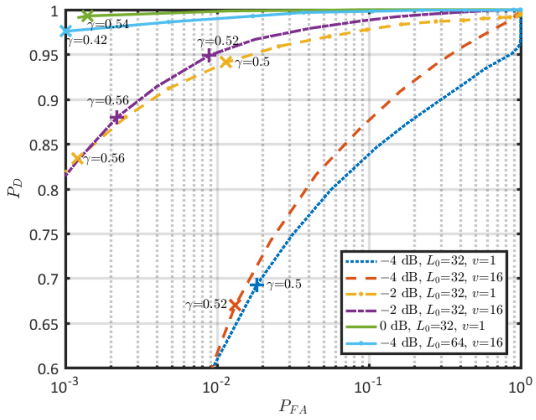

Fig. 4. Receiver operating characteristics (ROC) of the sequential detector

The SL estimators do not approach the CRVB [10] while the NM does. We also see the NM estimator gains a good accuracy based on the starting point of SL with v=16 at lower SNR due to the latter provides an enough accuracy. In contrast, the NM estimator based on SL with v=1 has worse accuracy than SL at all negative SNRs because the accuracy of SL is not enough so that the Newton iteration converges occasionally to other local minimum away from the real frequency offset.

Figure 3 compares the accuracy of our proposed estimators and the traditional estimators in [3]–[5]. It shows at the small frequency offset environment, our NM estimator even has a slightly better accuracy than traditional estimators at moderate SNRs. The drawback of NM estimator is also obvious that the accuracy depends on the SL. The figure also illustrates the lack of accuracy of single-lag estimators (our SL and Kay).

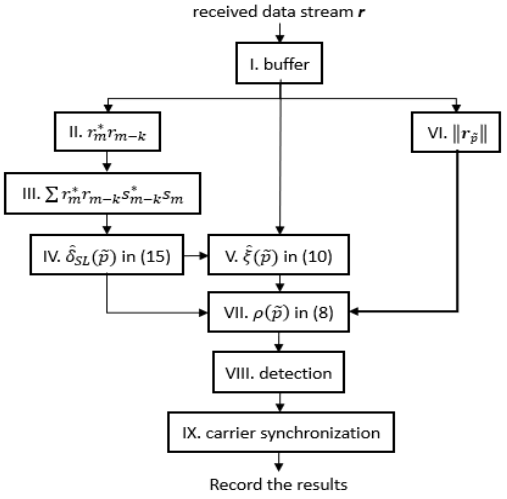

Fig. 5. Block diagram for implementing the proposed algorithm in FGI

B. Simulation Results for Detection

Figure 4 shows the receiver operating characteristics (ROC) of the detection algorithm. The better accuracy of SL with partial correlating at low SNRs also increases the performance of detection, e.g., at −2 dB SNR, $\gamma = 0.56$, the gap of false alarm probability P_{FA} is only 0.1% but the detection probability P_D of SL with v=16 is 5% larger than P_D of SL with v=1. The figure also shows the detector doesn't work well at −4 dB SNR if only 32 symbols of preamble are used; The performance is significantly improved by doubling the number of symbols.

VI. Implementation on Software-defined radio

To make our proposed algorithm work at a very high sample rate, the first improvement of algorithm is by using pipeline. Threading Building Blocks (TBB) is a well-known C++ library that enables parallel programming on multicore processor [11]. The Flow Graph interfaces (FGI) in TBB [11, Ch. 3] can make the algorithm implemented in a simple structure by seperating the algorithm into small nodes, which is used in this paper.

Figure 5 shows a simple block diagram for implementing the algorithm in FGI. Due to space constraints, we don't give all the details of each node but it is necessary to discuss about the node of computing phasor estimate $\hat{\xi}$ (node V). Note, the numerator of (10) performs like a time-varying convolution, which cannot be computed efficiently as by FFT. The solution to increasing the computation efficiency is by using parallel programming of TBB (or FGI). Specifically, (10) can be computed in three stages: 1. Compute several segments of $\sum r_n s_n^*$ in several nodes in parallel; 2. each node is then multiplied by $\hat{\delta}_{SL}$ at the middle index of the partial correlation. 3. Sum all the nodes together. Thus, (10) is computed more efficiently as

$$||\boldsymbol{s}||^2 \cdot \hat{\xi} \approx \sum_{i=0}^{L-1} e^{-j\pi\hat{\delta}\frac{N(2m+1)}{L}} \sum_{n=mN/L}^{(m+1)N/L-1} r_n s_n^*, \qquad (22)$$

where L is the number of nodes. Thus, by using parallel programming, the efficiency of computing $\hat{\xi}$ is increased by L^2.

TABLE II
Benchmark results of nodes in Figure 5 with buffer size 8192

Node name	Time (ns)	CPU (ns)	Iterations
I. Buffer	408721	407754	1703
II. $r_m^* r_{m-k}$	160069	160054	3416
III. $r_m^* r_{m-k} s_{m-k}^* s_m$	498967	498876	1471
IV. $\hat{\delta}_{SL}$	187135	187121	3602
V. $\hat{\xi}$	780620	780523	886
VI. $\|\|\boldsymbol{r}\|\|$	203907	203892	3416
VII. $\rho(\tilde{p})$	837253	837048	829
VIII. detection	378793	378765	1844
IX. carrier synchronization	811747	811739	844

Now we show the results of the proposed algorithm in parallel programming on SDR. The signal are transmitted and received between two universal software radio peripheral (USRP) connecting by a 5-Gigabit Ethernet cable. At the receiver side, the CPU includes 6 cores and 12 threads. The results of google benchmark for each node in Figure 5 are shown in Table II. Note, the time cost in the table should refer to one buffer size, i.e., 8192, and the throughput of the pipeline is determined by the node with the longest time. Thus, the ideal throughput is approximately equal to $8192/837253 \cdot 10^3 \approx 9.78$ MHz.

Based on the above discussion, we finally test the proposed algorithm at sample rate 10 MS/s. As a result, the throughput of the algorithm is in the range of 4.5 MS/s ∼ 5.0 MS/s with latency near 1 ms; The detection algorithm is very robust that the false alarm probability is near 0 at moderate SNR.

References

[1] D. D. Falconer, F. Adachi, and B. Gudmundson, "Time division multiple access methods for wireless personal communications," *IEEE Communications Magazine*, vol. 33, no. 1, pp. 50–57, 1995.

[2] M. Morelli and U. Mengali, "Feedforward frequency estimation for PSK: A tutorial review," *European Transactions on Telecommunications*, vol. 9, pp. 103–116, 1998.

[3] S. Kay, "A fast and accurate single frequency estimator," *IEEE Transactions on Acoustics, Speech, and Signal Processing*, vol. 37, no. 12, pp. 1987–1990, 1989.

[4] M. P. Fitz, "Further results in the fast estimation of a single frequency," *IEEE Transactions on Communications*, vol. 42, no. 234, pp. 862–864, 1994.

[5] M. Luise and R. Reggiannini, "Carrier frequency recovery in all-digital modems for burst-mode transmissions," *IEEE Transactions on Communications*, vol. 43, no. 2/3/4, pp. 1169–1178, 1995.

[6] B. Ramakrishnan, "Frame synchronization with large carrier frequency offsets: Point estimation versus hypothesis testing," in *2010 7th International Symposium on Communication Systems, Networks Digital Signal Processing (CSNDSP 2010)*, pp. 45–50, 2010.

[7] M. Chiani and M. Martini, "On sequential frame synchronization in awgn channels," *IEEE Transactions on Communications*, vol. 54, no. 2, pp. 339–348, 2006.

[8] Y. Liang, D. Rajan, and O. E. Eliezer, "Sequential frame synchronization based on hypothesis testing with unknown channel state information," *IEEE Transactions on Communications*, vol. 63, no. 8, pp. 2972–2984, 2015.

[9] M. Fitz, "Planar filtered techniques for burst mode carrier synchronization," in *IEEE Global Telecommunications Conference GLOBECOM '91: Countdown to the New Millennium. Conference Record*, pp. 365–369 vol.1, 1991.

[10] F. Gini, R. Reggiannini, and U. Mengali, "The modified cramer-rao bound in vector parameter estimation," *IEEE Transactions on Communications*, vol. 46, no. 1, pp. 52–60, 1998.

[11] J. R. Michael Voss, Rafael Asenjo, *Pro TBB: C++ Parallel Programming with Threading Building Blocks*. 2019.